# Sheffield Hallam University

# Physical and tribological properties of Nitrided AISI 316 stainless steel balls

YANG, Shicai, LUO, Quanshun, SUN, Hailing, KITCHEN, Matthew and COOKE, Kevin

Available from Sheffield Hallam University Research Archive (SHURA) at:

http://shura.shu.ac.uk/14131/

## Published version

## Repository use policy

# Physical and Tribological Properties of Nitrided AISI 316 Stainless Steel Balls

Shicai Yang[1], Quanshun Luo[2], Hailin Sun[1], Matthew Kitchen[2] and Kevin Cooke[1]

[1]*Teer Coatings Ltd., Miba Coating Group, West Stone House, Berry Hill Industrial Estate, Droitwich, WR9 9AS, UK*
[2]*Materials and Engineering Research Institute, Sheffield Hallam University, Howard Street, Sheffield S1 1WB, UK*

**Abstract.** AISI 316 austenitic stainless steel balls (diameters 5.0 and 12.0 mm, typical hardness 250 $HV_{0.3}$) and flat samples (20×20×2.0 mm) were nitrided by a pulsed glow discharge $Ar/N_2$ plasma. Hardness of the ball surfaces was analysed using Vickers indentation. Thermal stability of the nitrided balls (diameter 12.0 mm) was studied using a furnace to heat them in air for 8 hours at temperatures up to 700.0 °C and then, after cooling to room temperature, the surface hardness of the heated balls was re-measured. Scanning electron microscopy and X-ray diffraction were used to study the microstructures, composition and phase formation of the nitrided sublayers. Unlubricated pin-on-disc wear testing was used to evaluate the wear resistance of nitrided stainless steel balls (5.0 mm diameter) and the results were compared with similar testing on hardened Cr-Steel balls (5 mm diameter with hardness of about 650 $HV_{0.3}$). All the test results indicated that the nitrided AISI 316 austenitic stainless steel balls have advantages over the hardened Cr-Steel balls in terms of retaining high hardness after heat treatment and high resistance to sliding wear at room temperature under higher counterpart stress. These properties are expected to be beneficial for wide range of bearing applications.

## 1 Introduction

Austenitic stainless steels are known to have outstanding toughness, biomedical compatibility, corrosion resistance and oxidation resistance [1, 2], and therefore have been widely used in industries, such as food [3], biomedical devices [4-6], petroleum and chemical engineering [7], steam turbines [2], and nuclear energy generation [8]. A recent review of the composition, microstructure and functions of stainless steels can be found in Ref. [9]. The major weakness of austenitic stainless steels is their low hardness [10], typically 150 – 250 HV, which limits the wear resistance of components such as ball bearings. The surface hardness of stainless steel can be enhanced significantly to 1000 HV by means of nitriding treatments in a gaseous or plasma medium [11, 12]. These enable the production of piston rings and gears with outstanding tribological properties. Moreover, surface nitrided stainless steel could also find applications in ball bearings to be used at elevated temperatures owing to the material's combined high surface hardness and excellent oxidation resistance. To date, however, little research has been published on the plasma nitriding of austenitic stainless steel balls. One factor may be the complexity involved in supporting multiple balls while achieving an effective plasma treatment, and to provide uniform nitriding over the entire ball surface.

In this paper, we report recent research on the characterization and tribological evaluation of plasma nitrided balls made from austenitic stainless steel AISI 316, to explore its feasibility for ball bearing applications.

## 2 Experimental

Austenitic stainless steel AISI 316 was employed in the research, including balls of both 5 mm and 12 mm in diameter and square flat samples of 20 × 20 × 2.0 mm in size. The balls were manufactured with a grade 10 surface finish and the flat samples were manually polished with 1200# SiC abrasive paper, all samples being ultrasonically cleaned in acetone and dried before plasma treatment.

The nitriding treatment was completed using an industrial pulsed DC glow discharge plasma process [13], at input power 2.5 kW, pulse frequency 360 kHz and potential -550 V The gaseous medium in the nitriding chamber was controlled at a pressure of 1.33 Pa and with an $Ar/N_2$ flow ratio of 1:3. The nitriding process was controlled in a range 450 – 500 °C. In the nitriding chamber, each ball was supported with a specially made jig to ensure effective exposure to the nitriding atmosphere for most of the spherical surface, except a small area hidden by the jig, Fig. 1. After the first 3-hour nitriding process, the chamber was vented to atmosphere and each ball was turned by an angular rotation sufficient to allow the hidden area to be nitrided in a second 3-hour nitriding process.

**Figure 1.** A photograph taken inside the nitriding chamber, showing balls supported on the individual jigs.

A field emission SEM, FEI Nova-200 FEG-SEM, was employed to analyse the as-nitrided surfaces and cross-sectional microstructure. For the latter, cross-sectioned samples were ground and polished to mirror finish before chemical etching in a Kailling's No. 2 solution. Energy dispersive X-ray (EDX) spectroscopic chemical analysis was also applied along with the SEM observation. A Philips X'Pert X-ray diffractometer with radiation Cu-K$_{\alpha 1}$ ($\lambda$ = 0.154056 nm, at power of 40 kV and 40 mA) was employed to analyse the crystallographic properties.

The hardness properties were measured using two methods, namely, Vickers hardness of the nitrided surfaces at a load of 0.3 kg and Knoop hardness profile on polished cross-sections at an indenting load of 0.025 kg. The depth of the nitrided layers was measured on polished cross-sections using both SEM and optical microscopy.

Pin-on-disk sliding wear tests were carried using two configurations by using the nitrided ball samples and hardened Cr-steel balls with hardened and ground M42 tool steel flat samples as the counterpart. The wear tests were conducted at a constant applied normal load of 5 N and linear sliding speed of 0.2 m·s$^{-1}$. Each test ran for 60 minutes, before the ball and flat samples were taken off to measure the wear volumes.

# 3 Results and discussion

## 3.1 Microstructural characterization

The as-nitrided surface is shown to be slightly rougher than the as-polished surface, in Fig. 2a, as a result of lattice expansion induced plastic deformation of the austenitic grains. Some details of the crystalline slips are shown in the inserted image at higher magnification. Fig. 2b shows an etched cross-section of the nitrided layer, in which the nitrided layer can be recognised with a clear interface to the austenite substrate, associated with the deep-etching line near the centre of the image.
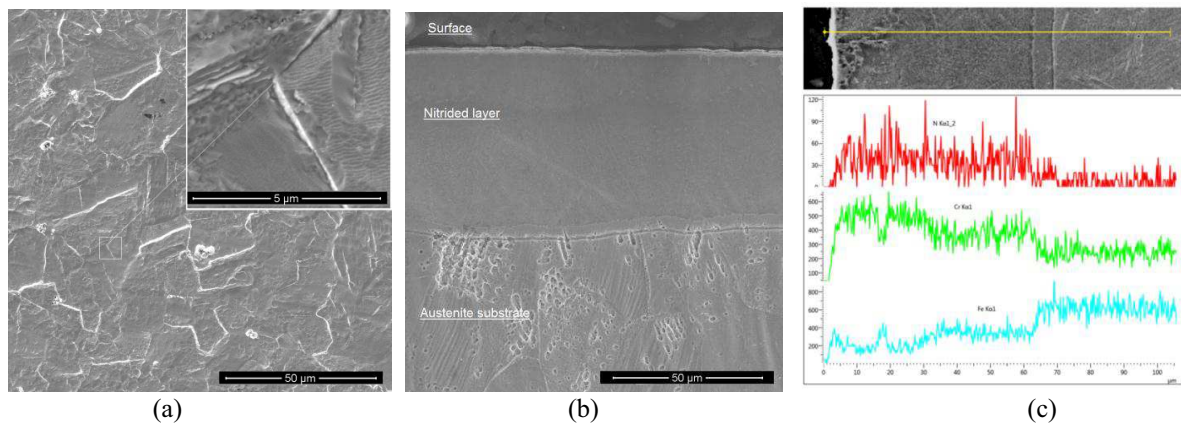


(a)                      (b)                      (c)

**Figure 2.** SEM and EDX analyses of the nitrided AISI316 steel ball: (a) As-nitrided surface; (b) Polished and chemically etched cross-section; and (c) EDX line scans of the N, Cr and Fe concentrations.

**Table 1** Chemical composition of nitrided surface determined by SEM-EDX.

|      | N     | Cr    | Mo   | Fe    | Ni    | Si   | Mn   |
|------|-------|-------|------|-------|-------|------|------|
| at%  | 26.77 | 13.77 | 0.87 | 48.68 | 8.03  | 0.84 | 1.05 |
| wt%  | 8.43  | 16.11 | 1.87 | 61.16 | 16.60 | 0.53 | 1.30 |

Fig. 2c is the line-scan profiles of the characteristic X-rays N-K, Cr-K and Fe-K, to show the variation of N, Fe and Cr concentrations in the nitrided layer. The line-scans indicate a distinct profile of nitrogen in the nitrided layer, along with enriched Cr and reduced Fe concentration in comparison to the austenite substrate, which supports the Cr-trapping nitriding mechanism [9]. Meanwhile, EDX analysis also reveals the chemical compositions of the

nitrided layer (acquired on the sample surface), in Table 1. Note that the N concentration is double that of the Cr concentration, indicating highly supersaturated nitrogen.

Fig. 3 shows X-ray diffraction curves of the nitrided and as-polished samples. The nitrided sample shows strong diffraction peaks of both the {111} and {200} planes as evidence of a substantially expanded austenite lattice (also called the S-phase [6, 9, 11]). In addition, several low-intensity diffraction peaks suggest precipitation of Cr- and or Fe-nitride phases.

## 3.2 Thickness, hardness property and thermal stability

To evaluate the thickness profile of the nitrided balls, a ball was sectioned diametrically across the region of the jig-obscured circle, and subsequently mounted, ground

and polished. The nitrided layer depth was measured at equal intervals of around 1 mm with a total of 22 readings between the minimum 46.43 μm and the maximum 59.03 μm, leading to a statistical average of 54.25 ± 3.29 μm. The measurements indicate a relatively uniform thickness distribution throughout the ball surface, whereas the jig-obscured area shows a reduced layer thickness of 39.73 ± 2.25 μm. Fig. 4 shows hardness profiles across the whole nitrided depth. The nitrided layer exhibits high hardness of $HK_{0.025}$ 1100-1200. It also shows that, the double 3-hour nitriding process brought about only a marginal further increase in the hardness.
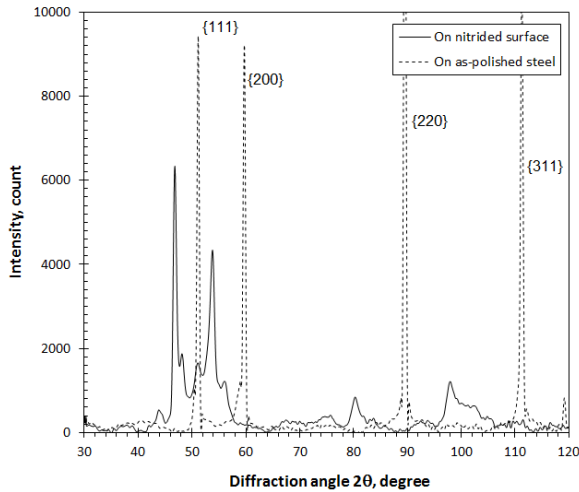


**Figure 3.** X-ray diffraction curves of nitrided and as-polished 316 steel samples.
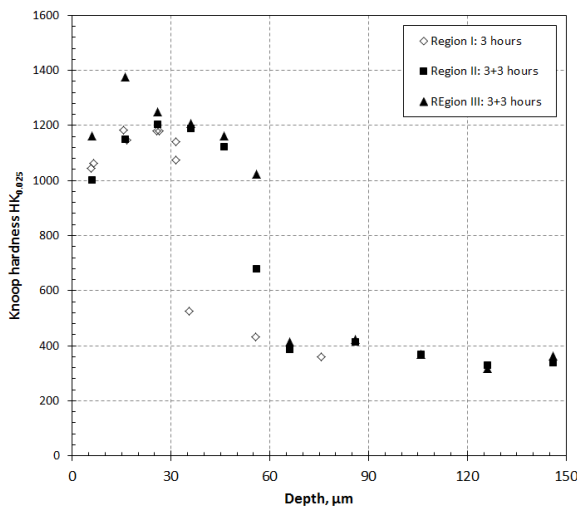


**Figure 4.** Microhardness depth profiles of as-nitrided ball.

Selected ball samples of both the nitrided 316 steel and hardened 100Cr steel were subjected to annealing treatments for 8 hours in air at an elevated temperature between 300 to 700 $^{o}$C. After the annealing treatments, Vickers' hardness was measured on the ball surface, as shown in Fig. 5. The hardness of the 100Cr steel dropped significantly from over HV 600 to below HV 400 following the tempering transformation of its martensitic structure. In contrast, the nitrided 316 steel maintained high hardness when the annealing temperature was up to

500 $^{o}$C, while the hardness was decreased when the annealing temperature was increased from 500 to 700 $^{o}$C. The different hardness properties of the annealed balls are also shown in Fig. 6. In Fig. 6, the hardness profile of the 300 $^{o}$C annealed nitrided ball was comparable to the as-nitrided ball, while annealing at 500 $^{o}$C resulted in a hardness drop at a depth of about 20 μm. The hardness of the 700 $^{o}$C annealed sample was significantly reduced. Nevertheless, the nitrided 316 steel exhibited superior thermal stability when compared to hardened 100Cr6 ball bearing steel, which implies its potential suitability for bearing components to be used at elevated temperatures.
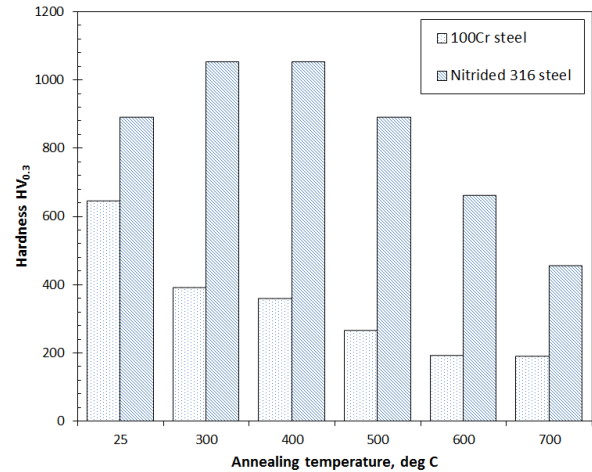


**Figure 5**. Effect of annealing temperature on the hardness property of nitrided 316 steel and hardened 100Cr steel.
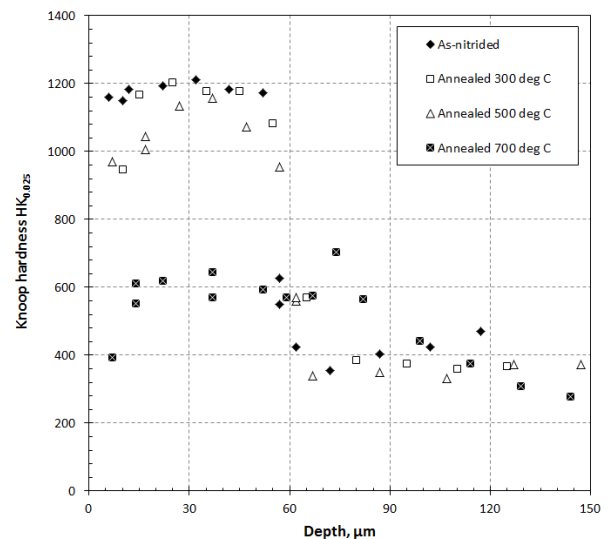


**Figure 6.** Microhardness depth profiles of as-nitrided and annealed balls.

## 3.3 Wear and friction properties

Details of the wear properties are summarised in Table 2. The 100Cr steel exhibited 12 times higher wear rate than the nitrided 316 steel when the applied load was 2 N. When the load was 5 N, the two "as received" materials' wear rates were more similar whereas the wear of the nitrided 316 was still four times lower.

**Table 2** Wear depth (*d*) and specific wear rate (*k*) of the tested samples

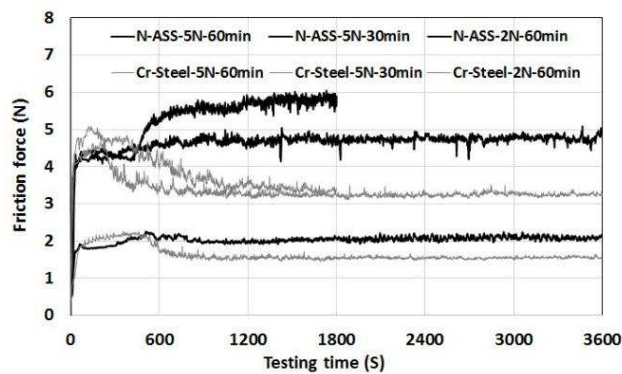| balls | $d_{ball}$ (μm) | $k_{ball}$ ($m^3$/Nm) | $k_{disc}$ ($m^3$/Nm) |
|---|---|---|---|
| At 5 N, run for 60 minutes | | | |
| N-ASS | 37.2 | $3.1×10^{-15}$ | $4.3×10^{-16}$ |
| Cr-Steel | 78.2 | $1.4×10^{-14}$ | $2.6×10^{-16}$ |
| At 5 N, run for 30 minutes | | | |
| N-ASS | 23.7 | $2.5×10^{-15}$ | $6.2×10^{-16}$ |
| Cr-Steel | 52.6 | $1.2×10^{-14}$ | $4.2×10^{-16}$ |
| At 2 N, run for 60 minutes | | | |
| N-ASS | 19.2 | $2.0×10^{-15}$ | $1.1×10^{-15}$ |
| Cr-Steel | 66.2 | $2.4×10^{-14}$ | $6.1×10^{-16}$ |



**Figure 7**. Friction corves of the tested samples.

Fig. 7 shows a collection of friction curves acquired in the ball-on-disk wear tests, in which "N-ASS" stands for nitrided 316 austenitic stainless steel and "Cr-Steel" for hardened 100Cr steel. The first test was carried out at an applied load 5 N for a total sliding time of 60 minutes, when the nitrided layer was worn through resulting in wear of the substrate. The sliding time was then reduced to 30 minutes to ensure that wear was limited to within the nitrided depth. Regardless of the applied loads and sliding distances, both the nitrided 316 and hardened 100Cr6 steels exhibited high friction coefficients, which could be explained by the adhesive steel-to-steel contact which occurred without the presence of lubrication.

Fig. 8a shows low-magnification images of the resulting wear scars. The wear rates of the nitrided 316 and 100Cr were dramatically different. Fig. 8b is the worn surface observed by SEM at high magnification, taken in the region of worn scar on nitrided ball after 60-minute and 5-N test. The SEM observation indicates that the rubbed nitrided ball surface exhibits typical sliding wear mechanisms of grooving deformation. Such wear is normally caused by hard abrasive particles. In this case, it is believed that the un-dissolved carbide particles in the high-alloy M42 tool steel should have played the role of hard abrasives, causing abrasive wear. When such wear mechanism dominates the sliding wear process, the wear rate decreases with the increase of hardness of the tested material, which can explain the striking difference between the wear rates of the nitrided 316 steel and the hardened 100Cr6. Fig. 9 shows the wear measurements of the counterpart M42 tool steel disks.
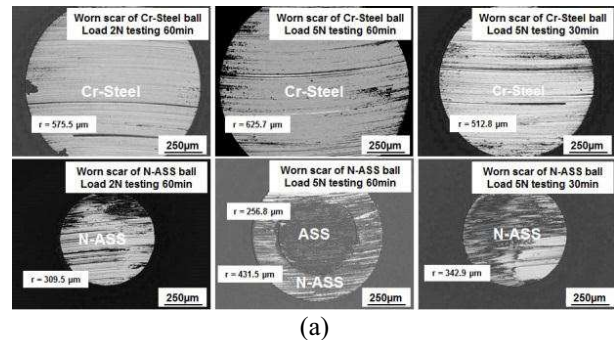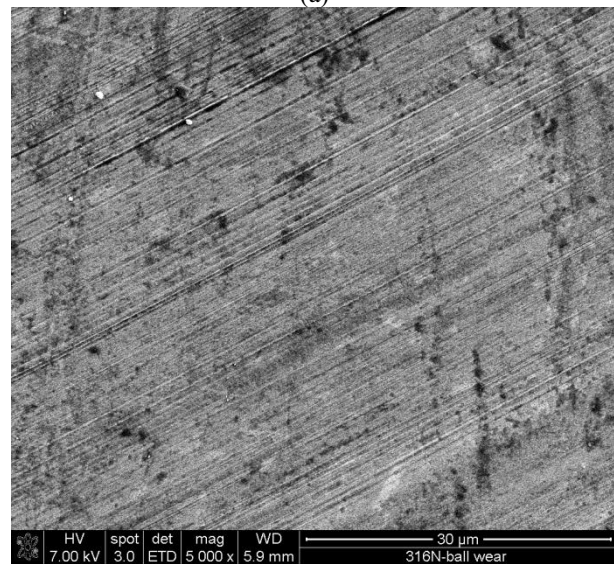


**Figure 8.** (a) Low magnification images of ball wear scars of nitrided 316 steel and hardened 100Cr steel; (b) A high magnification SEM image of the worn surface of the nitrided 316 ball.
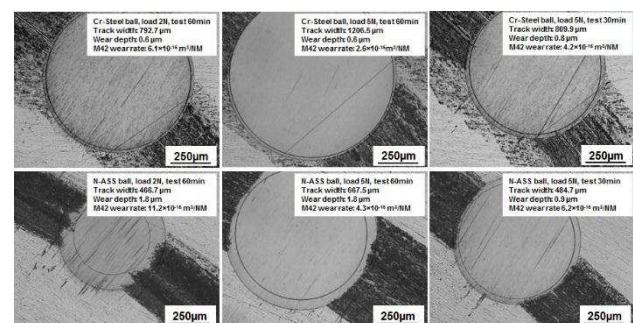


**Figure 9.** Low magnification images of the ball-crater measurements on wear tracks of the counterpart M42 steel disks.

The dramatically increased wear resistance of the nitrided 316 steel can be related to its increased hardness and hence increased resistance to abrasive wear and plastic deformation, and also by its enhanced thermal stability which helped to prevent softening due to the frictional heating. Further detailed investigation of the worn surfaces, e.g. by SEM examination, will be carried out later.

The main motivation of this work was to investigate the possibility that plasma nitrided austenitic stainless steel would be suitable for bearing applications. The results achieved so far do support the suggestion that, the combination of a hard and strong shell with a soft and

tough core can provide significantly improved wear resistance. The sliding wear performance of the nitrided steel balls was significantly better than that of the hardened 100Cr steel balls under identical testing parameters. Meanwhile, it is also noteworthy that the nitrided balls caused more wear of the counterpart M42 steel than the hardened 100Cr steel balls. This could be attributed to the stress induced high wear on the counterpart surface. It was estimated according to load divided by ball worn scar area that the pressure at the counterpart surface for the N-ASS balls was two times higher than that for the hardened 100Cr steel balls. Obviously N-ASS balls were shown to have a higher capability to resist stress induced plastic deformation in an abrasive environment that would cause fatigue and eventually wear at sliding interface. It would be interesting to study the rolling tribology performance of the N-ASS balls but this will need to be addressed in further research.

## 4 Conclusions

Nitrided AISI 316 austenitic stainless steel balls were characterised as having high hardness, high capability to withstand stress and high sliding wear resistance and outperformed hardened Cr-Steel balls and hardened M42 steel discs under the identical pi-on-disc testing.

Up to a maximum hardness of $HV_{0.3}$ 1000 can be retained on the nitrided AISI 316 austenitic stainless steel balls at temperatures up to 400℃, whereas in comparison the hardness of hardened Cr-Steel balls was reduced from the $HV_{0.3}$ 650 of the original to $HV_{0.3}$ 350 after heat treated.

All the results indicated that AISI 316 austenitic stainless steel balls were significantly improved in their tribological properties after nitriding suggesting the potential applicability of these nitrided austenitic stainless steel balls in the ball bearing industry.

## References

1. C. Allen, A, ball, Wear **74**, 287-3905 (1981-1982).
2. P. J. Maziasz, B. A. Pint, J. P. Shingledecker, K. L. More, N. D. Evans, E. Lara-Curzio, *Proceedings of ASME Turbo Expo* (2004) 2.
3. S. Cvetkovski, M. Matyer. Eng. **18** 283-293(2012).
4. K. Bordjih, E. Y. Jouzeau, D. Mainard, E. Payan, J. P. Delagoutte, P. Netter, Biomaterials **17** 491-500(1996).
5. T. Newson, Stainless steels for hygienic applications, *BSSA Conference-Stainless solutions for a sustainable future. Magna Science Advanture Centre*, Sheffield (2003).
6. J. Buhagiar, T. Bell, R. Sammons, H. S. DongS. J Mater Sci **22**,1268-1278 (2011).
7. R.D. Kane, M.S. Cayard, Corrosion **98,** 1-28 (1998).
8. S. Baindur, Bulletin of the Canadian Nuclear Society **29** 32-38 (2008).
9. Q. Luo, S. Yang, Int. J. Nanomed Nanosurg **1.1** 1–10 (2015).
10. E. T. Akinlabi, S, A. Akinlabi, Int J. Mechanical, Aerospace, Industrial, Mechatronic, and Manufacturing Engineering **8** 256-261 (2014).
11. Y. Sun, T. Bell, Wear **218** 34 (1998).
12. V. Toshkov, R. Russev, T. Madjarov, E. Russeva, J. Achiev. Mater. Manuf. Eng. 25, 71-74 (2007).
13. S. Yang, K. Cooke, H. Sun, X. Li, K. Lin, H. Dong, Surf. Coat. Technol. **236** 2-7 (2013).